Parametric investigation of a hybrid vehicle's achievable fuel economy with optimization based energy management strategy

Ali Amini[*1], S. Çağlar Başlamışlı[2a], Bayramcan Ince[2b], Kerem Köprübaşı[3c]
and Selim Solmaz[4d]

[1]*Department of Mechanical Engineering, Ataturk University, 25240 Erzurum, Turkey*
[2]*Department of Mechanical Engineering, Hacettepe University, 06800 Ankara, Turkey*
[3]*Ford Otosan A.Ş., Sancaktepe, 34885 Istanbul, Turkey*
[4]*Department of Mechatronics Engineering, Near East University, 99138 Nicosia, TRNC*

Abstract. The hybrid electric powertrain is a robust solution that allows for major improvements in both fuel economy and emission reduction. In the present study, a through-the-road hybrid vehicle model with an electric motor driving the rear axle and an Internal Combustion Engine (ICE) driving the front axle has been constructed. We then present a systematic method for the determination of a real time applicable optimal Energy Management Strategy (EMS) for a hybrid road vehicle. More precisely, we compare the performance of rule-based EMS strategies to an optimization-based strategy, namely ECMS (Equivalent Consumption Minimization Strategy). The comparison is conducted in parallel with a parameterization of the size of the internal combustion engine and the implementation of a Continuously Variable Transmission (CVT) that allows following the line of best fuel economy. For the FTP-75 driving cycle, the constrained engine On-off control algorithm is shown to offer a 28% improvement potential of fuel consumption compared to the conventional internal combustion engine while the ECMS strategy achieves an improved potential of nearly 33%.

Keywords: parallel hybrid vehicle; energy management strategy; fuel consumption

1. Introduction

The increase observed in the number of road vehicles worldwide in transportation systems leads to constantly increasing emission levels besides depleting petroleum-based fuel resources (Schipper 2011). This fact emphasizes the need for systems that can achieve very low or zero

*Corresponding author, Ph.D. Student, E-mail: ali82amini@gmail.com
[a]Ph.D., E-mail: scaglarb@hacettepe.edu.tr
[b]M.Sc. Student, E-mail: canince7@gmail.com
[c]Ph.D., E-mail: kkopruba@ford.com
[d]Ph.D., E-mail: selim.solmaz@gmail.com

emission levels. To address this issue, researchers have focused on technical solutions based on the electrification of automotive drive systems. The efficiency of electric motors approaches 95% making them the ideal powertrain solution especially under transient (speed varying) driving conditions where the internal combustion engine (ICE) suffers from poor efficiency (Lu 2016). However, due to capacity limitations of the current battery technology and the fact that fossil fuels are expected to increase their share of electricity production to reach almost 70% by 2050, pure electric drive vehicles are not expected to gain worldwide acceptance in the near future. This is the main reason why alternative technologies for enhancing fuel efficiency were introduced. The most prominent alternative approach is the design of hybrid drive systems operating a combination of ICE and electric motors (Lanzi *et al.* 2011).

Many different control algorithms were proposed for the hybrid vehicle drivetrain to achieve the power demanded by the driver, while maximizing vehicle range, controlling the battery state of charge (SoC), and keeping the operating efficiency of the internal combustion engine at the highest possible level. Maximum State of Charge (SoC) control algorithms, thermostat (On-Off) control algorithm, constrained engine On-Off algorithm, Dynamic Programming (DP) and Equivalent Consumption Minimization Strategy (ECMS) are among the various control methods of hybrid vehicles (Koprubasi 2008).

Maximum SoC and thermostat control methods are part of rule-based algorithms; they operate on a set of rules defined by an analysis of power flow in the hybrid drivetrain, fuel efficiency maps of ICE, and heuristics. The maximum SoC control algorithm maintains a high battery SoC to ensure the delivery of sufficient power to the drivetrain to support frequent acceleration demand. In the stop-and-go driving mode, the battery tends to be depleted quickly, so this strategy emphasizes the use of ICE as the primary power source. The latter charges the battery whenever possible. Charging is continued until the SoC level exceeds a predetermined maximum level (Ehsani *et al.* 2001).

Regarding the thermostat or On-Off control strategy, the engine is turned off when the SoC approaches an upper limit and the battery provides for the full power demand. As the lower level of SoC level is reached, the ICE starts operating again to charge the battery. Some parameters like emissions, fuel efficiency, and the electric motor/generator characteristics can also be used to determine the triggering level of the ICE operation (Khajepour *et al.* 2014).

Dynamic Programming (DP) is a numerical method used to calculate the optimal operating condition of hybrid vehicles for a specific driving cycle. Because traffic and road conditions ahead of a vehicle are generally unknown, obtained results have a theoretical value only and DP cannot be applied online. Meanwhile, the ECMS control strategy employs an online optimization method to split demanded power between the ICE and the battery. The power split between these two sources is determined to achieve minimum fuel consumption by relating the energy consumption of the battery to an equivalent ICE fuel consumption. The equivalent total fuel consumption is set as an objective function and is minimized online (Liu and Peng 2008). A comparison between ECMS control algorithm and normal ICE operation in terms of fuel consumption is also available in the authors' previous study (Amini *et al.* 2016).

Several researchers proposed predictive and adaptive methods to enhance ECMS capability in different driving conditions. Musardo *et al.* (2005) introduced an adaptive ECMS algorithm where algorithm parameters are updated during vehicle travel using real time information. By taking real time road power request into account, the control parameter of interest (the "equivalence factor") was updated periodically and battery SoC was maintained within specified limits while fuel consumption was minimized. It was shown that an adaptive ECMS algorithm could give results

that are close to the optimal solution obtained from dynamic programming. In a study by Fu *et al.* (2011) the model predictive control framework was blended with information obtained from the Intelligent Transportation Systems (ITS). A real-time vehicle energy management system was established and the sensitivity of the proposed system to noise and error in the velocity profile prediction under different control approaches were investigated

Downsizing of power components is another topic to be considered in hybrid vehicle design. Boyalı *et al.* (2007) proposed a design methodology on sizing electric motors and investigated the effect of hybridization in the reduction of fuel consumption. Their results show that the proposed sizing approach is effective in determining the overall efficiency of hybrid vehicle architecture. Boyalı et al. (2006) also proposed transition rules between the two power sources to satisfy smooth transient switching and improve vehicle drivability.

In the present study, a through-the-road hybrid vehicle model has been constructed to calculate vehicle requested power for the FTP-75 driving cycle. The model consists of one electric motor that drives the rear axle and an internal combustion engine that drives the front axle. A CVT and a differential device constitute components of the front drivetrain system. Power source modelling were simplified by using related torque-speed maps for ICE and EM. Then, two kinds of control methods including constrained engine On-Off and ECMS controllers have been selected and their performances were compared. ECMS controllers were shown to provide fuel economy improvement over On-Off controllers.

2. Methodology

In this section, ECMS and Constrained On-Off energy management strategies are described.

2.1 ECMS analysis

2.1.1 Cost function and constraints

Equivalent energy minimization strategy for hybrid vehicle control is based on the key assumption that the lowest fuel consumption of vehicle is obtained throughout the entire journey if the instantaneous lowest fuel consumption is achieved. Mathematical description of this assumption can be shown in Eq. (1)

$$\int \text{Min}[\dot{m}_f(t)]dt \approx \text{Min}\int \dot{m}_f(t)dt \qquad (1)$$

$\dot{m}_f(t)$ is the instantaneous fuel consumption of ICE. It should be mentioned that there is no guarantee of capturing the exact optimum point in fuel consumption minimizing problem, but this method is usually able to give near-optimal results for practical applications. ECMS method utilizes a cost function as described in Eq. (2) to minimize the total energy consumption generated by contribution of both electric and thermal energy paths.

$$J_{ECMS} = \dot{m}_f(t) + s(t) \sum_{i}^{n} \dot{m}_{i,eqf}(t) \qquad (2)$$

In the above, $\dot{m}_{i,eqf}(t)$ is the equivalent fuel consumption of *n* electric motors, which contribute in hybrid power generation. $s(t)$ is a key parameter named as equivalence factor. The description of the energy requirement in terms of fuel consumption is the reason for employing

such a factor. The equivalence factor should be calculated separately for each driving cycle. According to Zhang *et al.* (2016), applying an equivalence value obtained for a certain driving cycle to another driving cycle can cause the battery to be quickly discharged or unnecessarily overcharged.

While Eqs. (1)-(2) are solved for every time step, some constraints should be considered (Paganelli *et al.* 2002). During power generation, ICE speed (w_{ice}) should stay in its practical operational range and ICE torque (T_{ice}) should be positive and less than the maximum producible value ($T_{ice,max}$). Electric Motor (EM) speed (w_e) and torque (T_e) generation must take place in their predefined operating range. Minimum constraint for EM torque generation ($T_{ice,min}$) can be negative in the case of regenerative braking. Eq. (3) summarizes these restrictions

$$w_{e,min} \leq w_e \leq w_{e,max} \tag{3}$$

$$0 \leq T_e \leq T_{e,max}$$
$$0 \leq w_{ice} \leq w_{ice,max}$$
$$T_{ice,min} \leq T_{ice} \leq T_{ice,max}$$

The requested power by the road is to be satisfied by the contribution of both ICE and EM. Power sharing task is controlled by the *u* parameter to ensure that requested power is satisfactorily provided. According to Eq. (4), *u* is defined as the fraction of EM power to total power

$$u(t) = \frac{P_e(t)}{P_f(t) + P_e(t)} \tag{4}$$

where $P_f(t)$ and $P_e(t)$ are power generated by ICE and EM, respectively.

EM uses the energy stored in the battery. During operation of the hybrid system, the expected State of Charge (SoC) of the battery must not go beyond pre-defined upper and lower limits (SoC_{min} *and* SoC_{max}) while the control *u* variable stays in the pre-defined range of $[-u_l, u_r]$.

$$SoC_{min} \leq SoC \leq SoC_{max} \tag{5}$$

$u(t)$=0 when the power of the hybrid system is provided by ICE alone in the pure thermal state. If the control variable converges to the u_r limit, some of the power generation is carried out by EM and the battery charge rate starts to fall. Maximum value of u_r is one, when the whole power production task is expected from EM. Otherwise, when the control variable approaches to the u_l value, some of the generated power by ICE is stored in battery via the EM and the battery SoC starts to increase.

Evaluation of the equivalence factor represents one of the main tasks of the ECMS algorithm. In fact, this value affects system behavior as follows: if $s(t)$ is too large, the use of electrical energy is punished and fuel consumption rises up. Conversely, if $s(t)$ is too small, the use of electrical energy is excessive and SoC is reduced.

2.1.2 Equivalence factor and SoC correction term

The calculation of $s(t)$ is divided into two steps. In the first step, two equivalence factors are defined for battery discharge and charge state, that are named as s_c and s_d respectively (Sciarretta *et al.* 2004). These factors are equivalent to the overall use of positive or negative (regenerative) electric energy at the end of a driving cycle. Consumption of electric energy on whole driving cycle can be converted to equivalent fuel energy by using s_c and s_d. To calculate s_c and s_d

values, the hybrid system is run for a certain driving cycle, with permissible constant u values. Throughout the cycle, the use of fuel energy $\bar{E}_f$ and electric energy $\bar{E}_e$ are recorded. These values represent the final values of the cumulative amounts of $E_f(t)$ and $E_e(t)$ related to produced energy by ICE and EM. Here, $E_f(t)$ is the energy supplied by ICE while $E_e(t)$ is the energy supplied by EM. Fig. 1 shows $\bar{E}_f$ as a function of $\bar{E}_e$ when the hybrid vehicle travels a certain driving cycle with constant u values. The slopes of trend lines in charging and discharging region determine s_c and s_d values respectively.

In a second step, the equivalence factor $s(t)$ is calculated as a function of s_c and s_d values during the driving cycle by defining a probability factor $p(t)$, Eq. (6).

$$s(t) = p(t)s_d + (1 - p(t)s_c) \tag{6}$$

During real-time processing, probability factor $p(t)$ is defined as,

$$p(t) = \frac{E_e^+(t)}{E_e^+(t) - E_e^-(t)} \tag{7}$$

$E_e^+(t)$ and $E_e^-(t)$ values indicate the maximum positive and negative extremes that the hybrid controller may encounter in the future time step. It can be seen in Fig. 2 that $E_e^+(t)$ and $E_e^-(t)$ are achieved when the controller takes extreme values u_r and $-u_l$ values as input. Therefore, $E_e^+(t)$ and $E_e^-(t)$ can be calculated as follows

$$E_e^+(t) = E_e(t) + \frac{u_r(\bar{E}_m - E_m(t))}{\bar{\eta}_e} - \lambda(\bar{E}_m - E_m(t)) \tag{8}$$

$$E_e^-(t) = E_e(t) - \bar{\eta}_e u_l(\bar{E}_m - E_m(t)) - \lambda(\bar{E}_m - E_m(t)) \tag{9}$$

Average efficiency of electric path for driving cycle can be calculated by $\bar{\eta}_e$ factor as follows

$$\bar{\eta}_e = \sqrt{\frac{s_{chg}}{s_{dis}}} \tag{10}$$

In Fig. 2, the instantaneous mechanical energy, that is transferred to the wheels, is shown by $E_m(t)$. The total mechanical energy transferred through the cycle is indicated by $\bar{E}_m$. λ is defined as the ratio of E_{e0} to $\bar{E}_m$ where E_{e0} is electrical energy usage in pure thermal state. E_{e0} is a non-zero number due to regenerative braking.

To sum up, Eqs. (6)-(10) indicate the procedure that is followed to evaluate $s(t)$ value from the energy point of view. To enforce battery SoC constraint (Eq. (5)) the concept of real equivalent factor is applied on $s(t)$ as follows (Koprubasi 2008).

$$s_{act}(t) = f_{soc}(SOC(t))s(t) \tag{11}$$

$s_{act}(t)$ is used by ECMS during real-time application. SoC correction function is taken in a form similar to Eq. (12)

$$f_{SoC}(SoC(t)) = \left(1 + \left(\frac{SoC_{ave} - SoC(t)}{SoC_{ave} - SoC_{min}}\right)^{2n_{SoC}+1}\right)\left(1 + \tanh\left(\frac{f_{SoC,I}(SoC(t))}{SoC_{th}}\right)\right) \tag{12a}$$

$$f_{SOC,I}(SoC(t)) = 0.99f_{SoC,I}(t - \Delta t) + 0.01(SoC_{ave} - SoC(t)) \tag{12b}$$
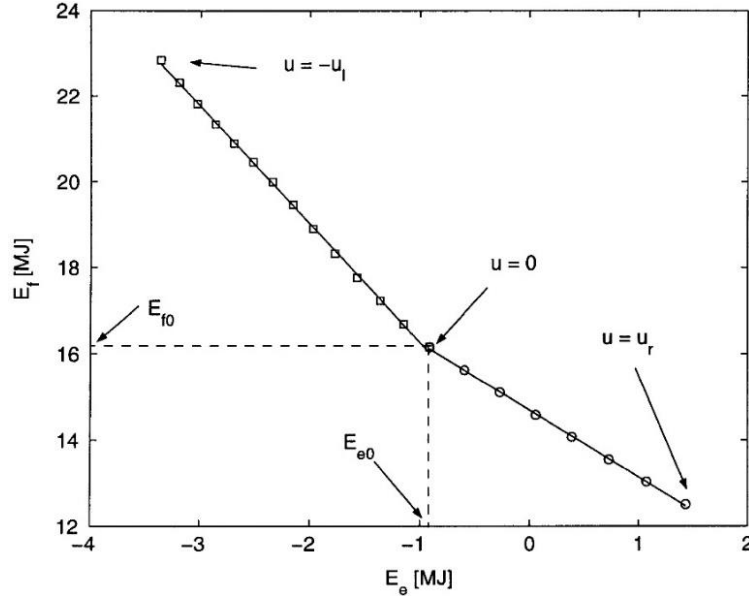
Fig. 1 Thermal energy vs electrical energy consumption for a sample driving cycle and for constant u steps (Sciarretta *et al.* 2004)
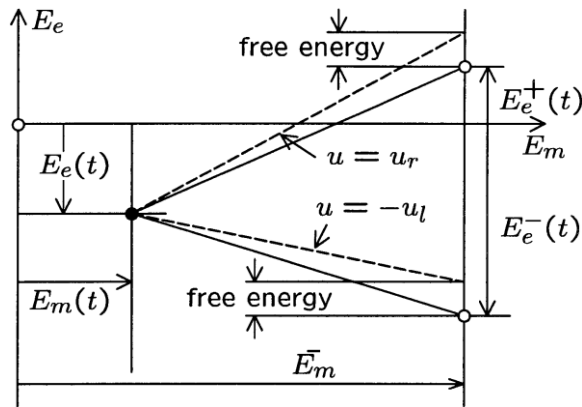

Fig. 2 Sketch of the quantities that lead to the evaluation of maximum positive and negative energy extremes (Sciarretta *et al.* 2004)

Battery SoC limits (average, minimum and maximum) used in the present work are as follows

$$\text{SoC}_{\text{ave}} = 65 \, \%$$ (13)

$$\text{SoC}_{\text{min}} = 60 \, \%$$
$$\text{SoC}_{\text{max}} = 70 \, \%$$

Here, Δt is the sampling time that is used to update the ECMS, $n_{SOC} \epsilon Z^+$ is a suitable function order, and SoC_{th} is the tolerance of the hyperbolic tangent function.

General form of problem definition in Eq. (1) can be rewritten for each time step Δt. The

control approach used in this paper finds the value of the control variable $u(t)$ by minimizing the cost function $J_{ECMS}(t,u)$, defined as (Sciarretta *et al.* 2004)

$$J_{ECMS}(t,u) = \Delta E_f(t,u) + s_{act}(t)\Delta E_e(t,u) \tag{14}$$

Quantities of $\Delta E_f(t,u)$ and $\Delta E_e(t,u)$ are the energy values supplied by thermal and electrical paths in the interval Δt. Both are functions of the control variable u and driving conditions, which are assumed to be constant over the time step Δt.

2.2 Constrained engine on-off control strategy

The constrained engine On-Off control strategy is a trade-off strategy between the maximum SoC and engine On-Off control strategies. More specifically, it is similar to maximum SoC method, however, requested traction torque levels are divided to low, medium and large torque regions; the operating regime of ICE is dependent on these torque regions. If the ICE operating point is below the established optimal efficiency line (economy line), it operates according to the specified throttle valve position by considering battery's SoC level. Table 1 and Fig. 3 show the operating states of the EM and ICE according to the battery SoC and torque demand (Ehsani *et al.* 2001). T_A, T_B and T_C are requested traction torques in large, medium, and low torque areas corresponding to point A, B, and C in Fig. 3. T_a, T_b and T_c are requested engine torques corresponding to point a, b, and c. T_{ch} indicates the electric component charging torque that is calculated by considering requested torque and battery SoC level.
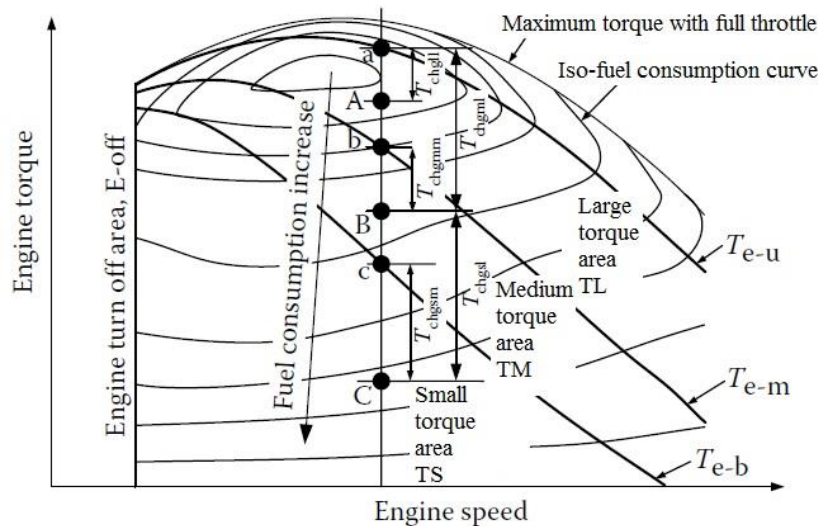

Fig. 3 Illustration of the constrained engine On-Off control strategy (Ehsani *et al.* 2001)

3. Mathematical modeling

3.1 Mathematical model of vehicle dynamics

Ali Amini et al.

Table 1 Constrained On-Off control strategy with different requested traction torque and battery SoC level

Request torque	Battery Low SoC area	Battery Medium SoC area	Battery High SoC area
Small torque area (point C)	$T_e = T_b$ $T_{chg-sl} = T_b - T_C$	$T_e = T_c$ $T_{chg-sm} = T_c - T_C$	$T_e = 0$ $T_{chg-sh} = 0$
Medium torque area (point B)	$T_e = T_a$ $T_{chg-ml} = T_a - T_B$	$T_e = T_b$ $T_{chg-mm} = T_b - T_B$	$T_e = T_B$ $T_{chg-mh} = 0$
Large torque area (point A)	$T_e = T_a$ $T_{chg-ll} = T_a - T_A$	$T_e = T_A$ $T_{chg-lm} = 0$	$T_e = T_A$ $T_{chg-lh} = 0$

The architecture of the parallel hybrid vehicle under study is shown in Fig. 4. In this study, one electric motor drives the rear axle and an internal combustion engine drives the front axle. A Continuous Variable Transmission (CVT) and a differential device constitute components of the front power transfer system. This configuration is called a *through-the-road parallel hybrid system*. The Matlab/Simulink environment has been used to create the vehicle model. The characteristics of the hybrid vehicle and powertrain system are given in the Appendix.

The longitudinal resistance forces acting on the vehicle are given in Fig. 5. Traction forces F_{xf} and F_{xr} are required to accelerate the vehicle. Total inertia torque of the rotating parts (that constitute the acceleration resistance), rolling and air resistance forces are calculated as described in Boyalı *et al*. (2006).

3.1.1 Rolling resistance
The rolling resistance force developed under each tire can be calculated by the following equation (Boyalı and Güvenç 2010)

$$F_r = P^\alpha W^\beta (a + bV + cV^2) \tag{15}$$

In the above equation, P represents the wheel pressure (kPa), W represents the load on the wheels (N), V represents the vehicle speed (m/s). a, b, c, α and β are the coefficients are obtained by experimental methods.
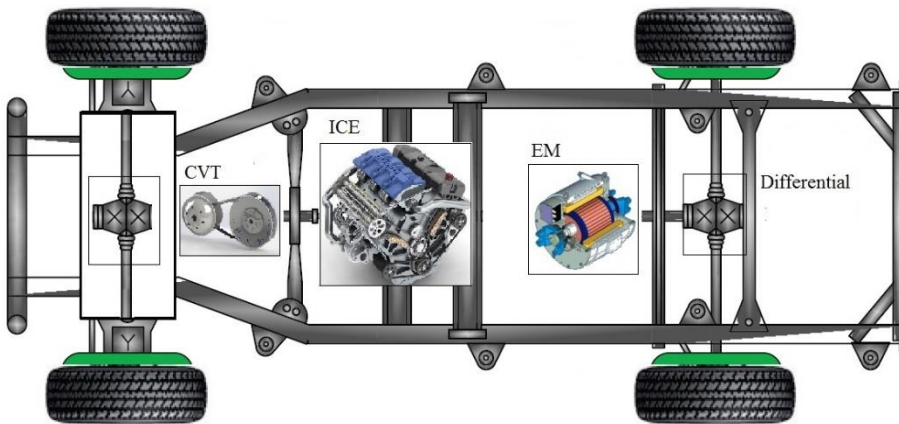

Fig. 4 Hybrid vehicle powertrain architecture

3.1.2 Aerodynamic resistance

Aerodynamic resistance is calculated as follows

$$F_a = \frac{1}{2} A\rho C_D V^2 \tag{16}$$

In the above equation, F_a is the aerodynamic resistance force (N), A is the frontal area of the vehicle (m²), ρ is the air density (kg/m³), C_D is the aerodynamic resistance coefficient (drag coefficient).

3.1.3 Inertial resistance and longitudinal vehicle dynamics

Besides road resistances, the engine traction forces and braking forces are imposed on wheels and contribute to the longitudinal vehicle dynamics. F_{xf} and F_{xr} are the total traction or braking forces acting on front and rear wheels. The longitudinal acceleration a_x of the vehicle is calculated as follows

$$F_t = \gamma m a_x = F_{xf} + F_{xr} - F_a - F_r \tag{17}$$

Since the vehicle has rotating masses, the total vehicle inertia is multiplied by the rotating mass factor γ. ICE, gearbox and differential inertia moments and gear ratio values are used in calculating the rotating mass factor. By using kinetic energy analysis, one can reduce the inertia of rotating masses to the wheels and the equivalent inertia is calculated as given (Boyalı and Güvenç 2010)

$$\frac{J_e w_e^2}{2} + \frac{J_p w_p^2}{2} + \frac{J_t w_t^2}{2} + \frac{mV^2}{2} = \frac{\gamma m V^2}{2} \tag{18}$$

$$\gamma m = m + \frac{\frac{J_e}{(i_g i_d)^2} + \frac{J_p}{(i_d)^2} + J_t}{R_e^2} \tag{19}$$

where J_e, J_p and J_t represent the ICE, differential and wheel inertia moments. i_g and i_d are gearbox and differential ratios. w represents rotational speed for every component.
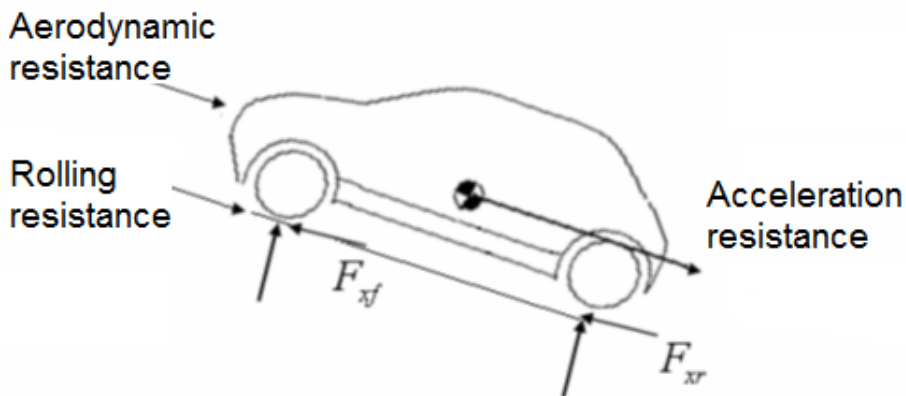

Fig. 5 Longitudinal forces acting on the vehicle (Boyalı *et al.* 2006)

3.2 Powertrain modeling

In the powertrain modeling process, fuel consumption and efficiency maps are used. It is also assumed that the thermal path includes an ideal CVT model. This means that the gear ratio is controlled automatically to track a specific line on the ICE map, called 'economy line'. Therefore, engine operating point can be optimized for any torque request to achieve best fuel economy. A typical petrol engine torque speed map with Specific Fuel Consumption (SFC) contours and constant power lines is shown in Fig. 6. Selection of the minimum fuel consumption for increasing output power gives the economy line. Hence, it is assumed that by equipping thermal path with a CVT device, it is possible to follow the economy line which ensures correct matching between engine condition and vehicle output speed (Julian 2002). For the electric path, a separate efficiency map which is a function of torque and angular speed of the motor has been used, while, in the battery model, an equivalent circuit diagram with internal resistances has been used. In this study, internal resistance of the battery has been taken as a function of battery SoC only. By calculating the resistance values according to the battery map, instantaneous current can be calculated according to

$$I_{chg} = \frac{-V_{oc} + \sqrt{V_{oc}{}^2 + 4R_i P_{chg}(t)}}{2R_i} \tag{20a}$$

$$I_{dis} = \frac{V_{oc} - \sqrt{V_{oc}{}^2 - 4R_i P_{dis}(t)}}{2R_i} \tag{20b}$$

where $P_{chg}(t)$, $P_{dis}(t)$ are charging and discharging loads in the battery terminal. V_{oc} is open circuit voltage and R_i is the internal resistance of battery.
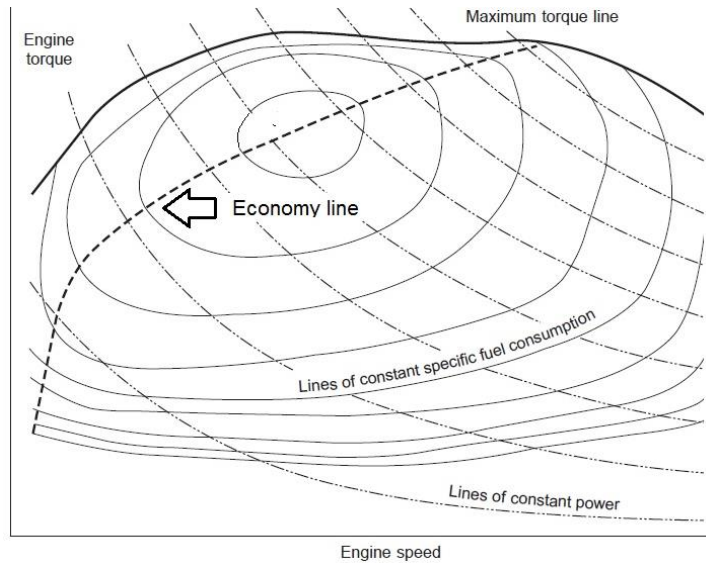

Fig. 6 Economy line on ICE Torque-Speed map (Julian 2002)

4. Simulation results

4.1 Thermal and electrical energy equivalence values

The Highway 'FTP-75' driving cycle has been selected for the implementation of the control algorithm (Fig. 7). Vehicle model was created in Matlab/Simulink environment and run for different u values in order to extract thermal energy and electric energy values during whole driving cycle for the ultimate aim of determining nominal s_c and s_d parameters. In this numerical experiment, values of u were reduced from 0.8 down to -1.0 by 0.1 steps. Values of $E_f(t)$ and $E_e(t)$ according to this changing parameter were shown in Fig. 8. Slopes of the trend lines give the values of s_c and s_d parameters used to convert the amount of electrical energy into thermal energy. Hybridization makes it possible to use different ICE scales in power generation. Fig. 8 shows four different ICE scales that yielded four different sets of s_c and s_d values. As a matter of fact, as the ICE scale is changed, engine operation point locations on speed-torque map are changed and does the efficiency. Therefore, fuel consumption value can be affected by engine downsizing. As a result, the slope of characteristic lines in Fig. 8 are changed.

Inspecting Fig. 8 reveals that at $(u = 0)$ point, EM runs as a generator. Electrical energy is found to be around -3 MJ at the fracture point of two lines. Also, it can be seen that for $(u = 0.25)$ the battery SoC remains constant throughout the cycle which means that total amount of energy taken from the battery and given to the battery is zero for this specific operating point.
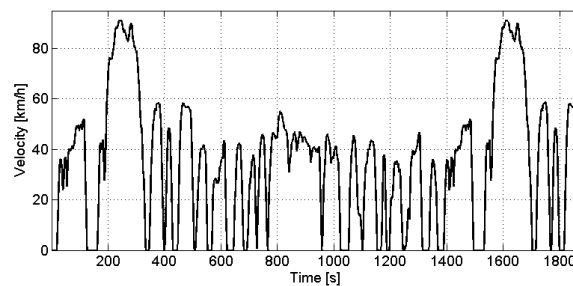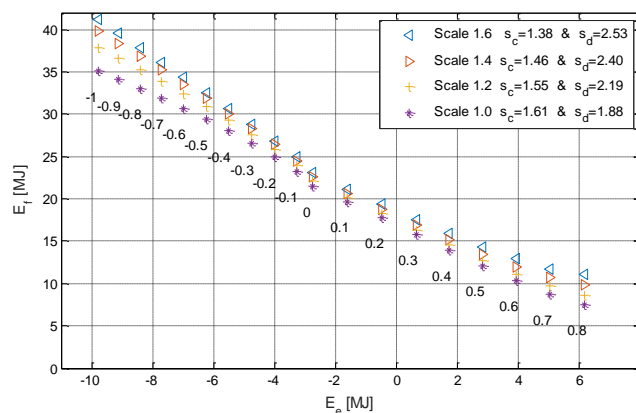

Fig. 7 FTP-75 driving cycle

Fig. 8 Thermal energy as a function of electrical energy obtained for the present driving cycle

4.2 Vehicle control by ECMS

During the implementation of the ECMS algorithm, related equations were calculated at a time step of 1 sec. and power sharing was established between power sources according to the optimum u value. Fig. 9(a) gives the ICE operation points on the torque-speed map. ICE operation points are conveniently below the engine maximum torque curve and they follow the economy line owing to the functioning of the CVT. Fig. 9(b) gives the EM operation points on torque-speed map. The distribution of points in this map shows that low torque request has been supplied by EM rather than ICE. Also, in deceleration cases, EM have been used to maximum energy recovery. Regarding the size of the EM, a suitable choice has been made in order to provide adequate traction force and regenerative braking force. Fig. 9(c) shows that the SoC of battery varies between 60% and 70%. The controller acted in such a way that battery charge level did not exceed the specified upper and lower limits. Summation of generated power by the ICE and EM during the driving cycle was compared to the requested road power calculated from the driving cycle speed profile in Fig. 9(d). The reason for the slight excessive power provided by hybrid powertrain is due to the efficiency of the powertrain.

(a) ICE operation points

(b) EM operation points

(c) Battery SoC

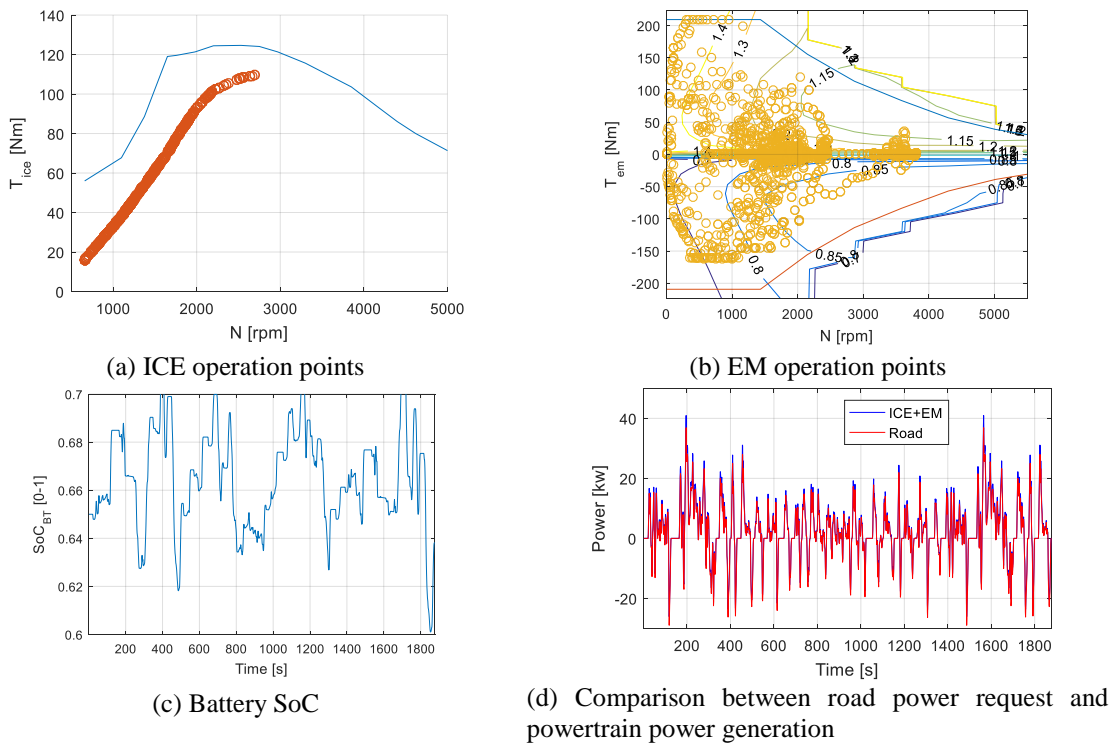(d) Comparison between road power request and powertrain power generation

Fig. 9 Performance of ECMS controller (engine scale=1.6)

4.3 Vehicle control by constrained on-off strategy

Next, the constrained engine On-Off control strategy has been implemented and compared with

ECMS strategy. Operating states of the EM and ICE was evaluated according to the battery SoC and torque demand listed in Table 1. Fig. 10(a) gives the location of ICE operation points on torque-speed map. In the small torque area, ICE operation was avoided unless SoC was small. Fig. 10(b) gives the EM operation points on torque-speed map. Distribution of points in this map shows that low torque requests was supplied by EM most of the time. Also, in the medium and large torque areas, EM power generation was rarely used. All the points are conveniently below the ICE and EM maximum torque curve. Variation of battery SoC can be seen in Fig. 10(c). SoC values of 0.625 and 0.675 are the separating lines that indicate battery's low, medium and high SOC zones. Finally, Constrained On-Off controller tends to maintain SoC values in medium SOC zones. A comparison between requested and generated power can be seen in Fig. 10(d).
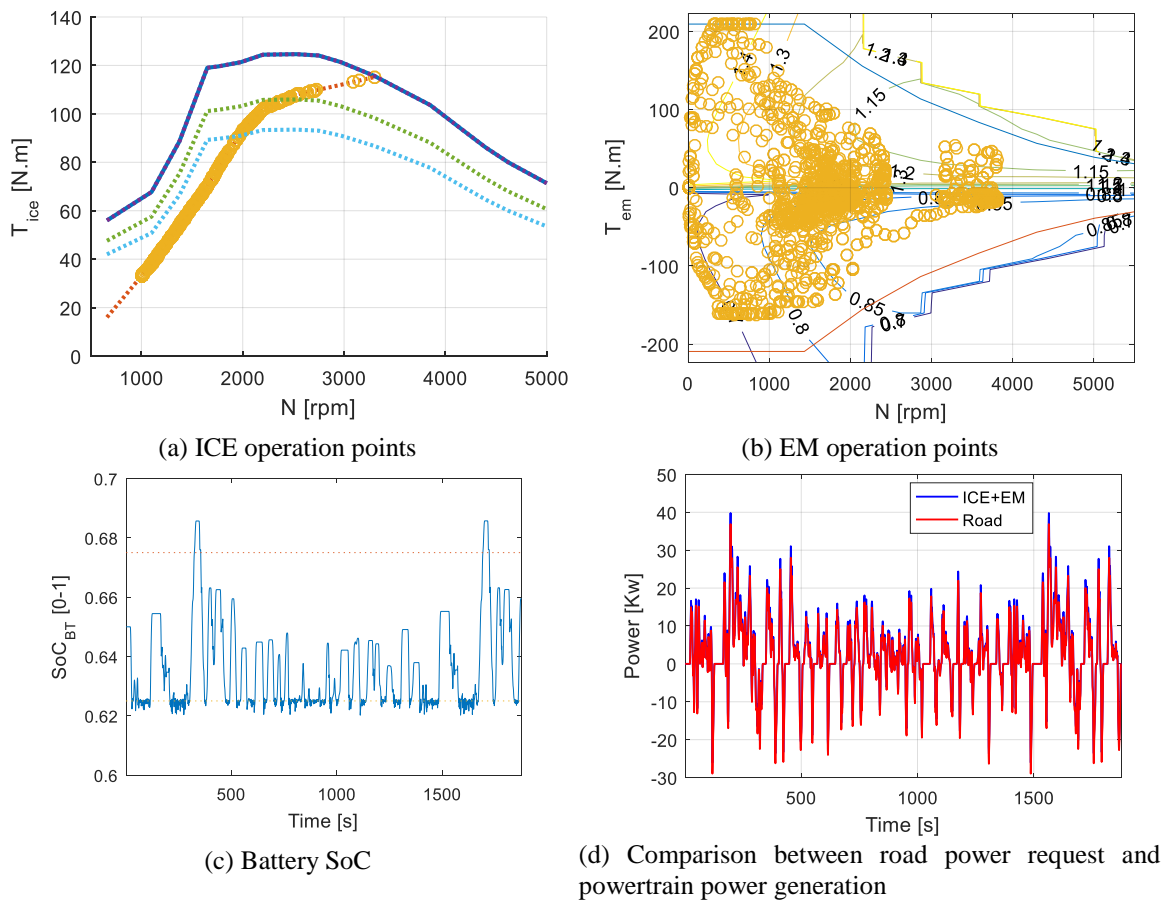

(a) ICE operation points

(b) EM operation points

(c) Battery SoC

(d) Comparison between road power request and powertrain power generation

Fig. 10 Performance of Constrained On-Off controller (engine scale=1.6)

4.4 Fuel consumption performance of hybrid driveline configurations

A comparison of fuel consumption performance for different arrangements of power sources is presented in Fig. 11 and Table 2. The highest value of fuel consumption belongs to the conventional vehicle that uses only ICE as a power source. Engine scale for this arrangement is 1.8
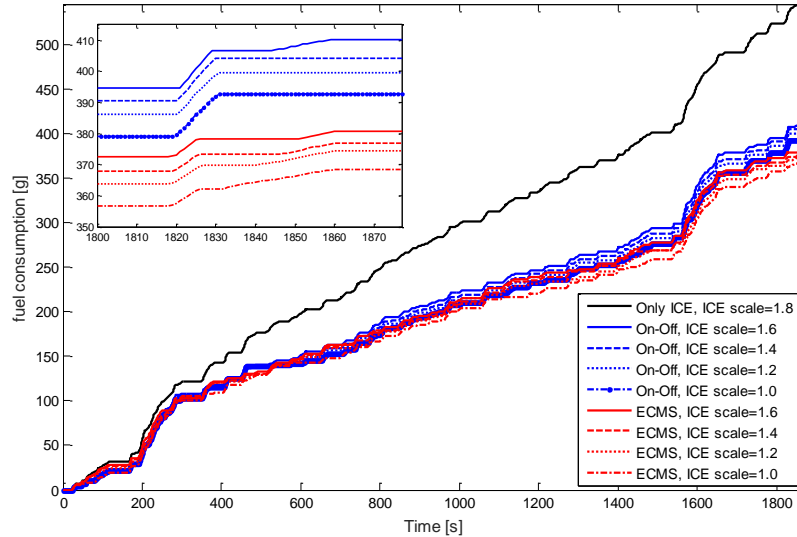
Fig. 11 Comparison of fuel consumption for different control methods

Table 2 Comparison of fuel consumption performance and battery final SoC for different control methods

Control strategy	ICE scale	Maximum torque (N.m)	Final SoC (%)	Fuel consumption reduction (%)
Only ICE	1.8	144	-	-
On-Off	1.6	128	65.95	24.85
On-Off	1.4	112	66.86	25.99
On-Off	1.2	96	67.80	26.83
On-Off	1	80	69.23	28.08
ECMS	1.6	128	63.82	30.40
ECMS	1.4	112	64.29	30.95
ECMS	1.2	96	64.88	31.50
ECMS	1	80	65.41	32.60

to produce a maximum torque of 144 (N.m) that is sufficient to satisfy road power request all over the driving cycle. Here, the unit scale represents an engine with maximum torque generation of 80 (N.m).

While implementing the hybrid structure, it is possible to downsize the ICE scale. The ICE scale was first downsized to 1.6 scale to produce a maximum torque of 128 (N.m), as was achieved in the scenarios presented in the previous sections. For these cases, constrained On-Off strategy provided a 24.85% reduction in fuel consumption compared to the conventional vehicle equipped with ICE only. Meanwhile, the ECMS controller made it possible to reach 30.40% reduction in fuel consumption.

It should be mentioned that fuel consumption comparison is fair only when a SoC level equal to the initial SoC level is obtained at the end of travel. So, a conversion factor is needed to convert part of extra energy that has been stored in battery. In this study, the conversion factor suggested by the United States Environmental Protection Agency (EPA) is used. The EPA considers 33.7 kWh of electricity is equivalent to one gallon of gasoline (Khajepour *et al.* 2014). The conversion

factor was used when obtaining results presented in Table 2. As a final case study, ICE scale was reduced down sequentially to 1.4, 1.2 and 1. As a result, maximum torque generation capability of engine reduced down to 112, 96 and 80 (N.m). Related values in Table 2 show that there was a gradual improvement in fuel consumption performance when ECMS together with correct engine scaling is used.

5. Conclusions

In the present study, we presented a systematic method for the determination of a real time applicable optimal energy management strategy for a hybrid road vehicle. Rule based On-Off and ECMS control strategies were compared. The comparison was conducted in parallel with a parametrization of the size of the internal combustion engine and the implementation of a CVT transmission that allows following the line of best fuel economy. ECMS controllers were shown to provide a huge improvement over rule-based controllers in terms of fuel economy: ECMS controller achieved a fuel consumption improvement of nearly 33% while the rule-based controller achieved an improvement of 28% only, which clearly indicates the benefit of using driving cycle information when designing hybrid EMS strategies. As a future work, the online determination of real world driving cycles and their incorporation in the design of the EMS strategies will be discussed.

Acknowledgments

Note

This paper is revised and expanded version of a paper entitled "Parametric investigation of a hybrid vehicle's achievable fuel economy with optimization based energy management strategy" presented at OTEKON2016, 8. Automotive Technologies Congress, Bursa, 23-24 May, 2016.

References

Amini, A., Önder, E.T., Başlamışlı, S.Ç., Köprübaşı, K. and Solmaz, S. (2016), "Parallel hybrid vehicle fuel consumption optimization by equivalent consumption minimization strategy", *Proceedings of the 8th Automotive Technology Conference, OTEKON,* Bursa, May.

Boyalı, A., Acarman, T. and Güvenç, L. (2007), "Component sizing in hybrid electric vehicle design using optimization and design of experiments techniques", *Proceedings of the Workshop on Hybrid Electric Vehicle Modeling and Control in connection with IEEE 2007 Intelligent Vehicle Symposium*, Istanbul, June.

Boyalı, A. and Güvenç, L. (2010), "Hibrid elektrikli araçların modellenmesi ve kural tabanlı kontrolü", *İstanbul Teknik Dergisi/D-Mühendislik*, **9**(2), 83-94.

Boyalı, A., Demirci, M., Acarman, T., Güvenç, L., Tür, O., Uçarol, H. and Özatay, E. (2006), "Modeling

and control of a four wheel drive parallel hybrid electric vehicle", *Proceedings of the International Conference on Control Applications*, Munich, October.

Boyalı, Y.M. (2008), "Hibrid elektrikli yol taşitlarinin modellenmesi ve kontrolü", Ph.D Dissertation; Istanbul Technical University, Istanbul, Turkey.

Ehsani, M., Gao, Y. and Emadi, A. (2001), *Modern Electric, Hybrid Electric, and Fuel Cell Vehicles, Fundamentals, Theory, and Design*, Taylor and Francis Group, Boca Raton, Florida, U.S.A.

Fu, L., Özgüner, Ü., Tulpule, P. and Marano, V. (2011), "Real-time energy management and sensitivity study for hybrid electric vehicles", *Proceedings of the American Control Conference*, San Francisco, July.

Julian, H.S. (2002), *An Introduction to Modern Vehicle Design*, Butterworth-Heinemann, Jordan Hill, Oxford Great Britain.

Khajepour, A., Fallah, S. and Goodarzi, A. (2014), "*Electric and Hybrid Vehicles Technologies, Modeling and Control: A* Mechatronic *Approach*", Wiley, Chi Chester, West Sussex, U.K.

Koprubasi, K. (2008), "Modeling and control of a hybrid-electric vehicle for drivability and fuel economy improvements", Ph.D. Dissertation, Ohio State University, Ohio, U.S.A.

Lanzi, E., Verdolini, E. and Hascic, I. (2011), "Efficiency-improving fossil fuel technologies for electricity generation: Data selection and trends", *Energy Pol.*, **39**(11), 7000-7014.

Liu, J. and Peng, H. (2008), "Modeling and control of a power-split hybrid vehicle", *IEEE Trans. Contr. Syst. Technol.*, **16**(6), 1242-1251.

Lu, S.M. (2016), "A review of high-efficiency motors: Specification, policy", *Renew. Sustain. Energy Rev.*, **59**, 1-12.

Musardo, C., Rizzoni, G. and Staccia, B. (2005), "A-ECMS: An adaptive algorithm for hybrid electric vehicle energy management", *Proceedings of 44th IEEE Conference on Decision and Control, and the European Control Conference*, Seville, December.

Paganelli, G., Delprat, S., Guerra, T., Rimaux, J. and Santin, J. (2002), "Equivalent consumption minimization strategy for parallel hybrid powertrains", *Proceedings of the IEEE 55th Vehicular Technology Conference*, Birmingham, May.

Sabri, M., Danapalasingam, K., Rahmat, M., Ridzuan, M. and Yusof, M. (2015), "Fuel economy analysis of through-the-road hybrid electric vehicle", *Proceedings of the Control Conference (ASCC)*, Kota Kinabalu, June.

Schipper, L. (2011), "Automobile use, fuel economy and CO_2 emissions in industrialized countries: Encouraging trends through 2008?" *Transp. Pol.*, **18**(2), 358-372.

Sciarretta, A., Back, M. and Guzzella, L. (2004), "Optimal control of parallel hybrid electric vehicles", *IEEE Trans. Contr. Syst. Technol.*, **12**(3), 352-363.

Zhang, F., Xi, J. and Langari, R. (2016), "Real-time energy management strategy based on velocity forecasts using V2V and V2I communications", *IEEE Trans. Intellig. Transport. Syst.*, **PP**(99), 1-15.

FO

Appendix

Table A1 Hybrid vehicle model and power supply specifications (engine scale=1.6)

Element	Parameters	Value
Vehicle	Design	Parallel hybrid
	Weight	1680 (kg)
	Air resistance coefficient	0.32
	Air density	1.24 (kg/m^3)
	Front side area	2.31 (m^2)
	Wheel radius	0.29 (m)
Transmission	Minimum Gear ratio	0.7/1
	Maximum Gear ratio	4.65/1
	Gear shifting	continuous
	CVT Efficiency	0.92
	Differential ratio	11/3
	Differential efficiency	0.92
Internal Combustion Engine	Fuel type	Gasoline
	Maximum torque	128 (N.m)
	Maximum power	72 (kW)
	Maximum speed	5200 (RPM)
Electric Motor	Maximum torque	210 (N.m)
	Maximum power	34 (kW)
	Differential ratio	4.57
	maximum speed	5700 (RPM)
Battery	Voltage	290 (v)
	Capacity	1 (Kwh)